Molecular Crystals and Liquid Crystals Science and Technology. Section A. Molecular Crystals and Liquid Crystals

Publication details, including instructions for authors and subscription information:
http://www.tandfonline.com/loi/gmcl19

Liquid, Glass, and Protein Vibrational Dynamics: Infrared Vibrational Echo Experiments

K. D. Rector [a] & M. D. Fayer [a]

[a] Department of Chemistry, Stanford University, Stanford, CA, 94305

Version of record first published: 04 Oct 2006.

To cite this article: K. D. Rector & M. D. Fayer (1996): Liquid, Glass, and Protein Vibrational Dynamics: Infrared Vibrational Echo Experiments, Molecular Crystals and Liquid Crystals Science and Technology. Section A. Molecular Crystals and Liquid Crystals, 291:1, 1-9

To link to this article: http://dx.doi.org/10.1080/10587259608042723

Mol. Cryst. Liq. Cryst., 1996, Vol. 291, pp. 1–9
Reprints available directly from the publisher
Photocopying permitted by license only

LIQUID, GLASS, AND PROTEIN VIBRATIONAL DYNAMICS: INFRARED VIBRATIONAL ECHO EXPERIMENTS

K. D. RECTOR and M. D. FAYER
Department of Chemistry, Stanford University, Stanford, CA 94305

ABSTRACT

The vibrational dynamics of polyatomic molecules in polyatomic liquids, glasses and proteins are examined using picosecond infrared vibrational echo experiments and pump-probe experiments as a function of temperature. The vibrational echo experiments measure T_2, the homogenous dephasing time, while the pump-probe experiments measure the vibrational lifetime, T_1, and orientational relaxation dynamics. By combining these measurements, a complete analysis of vibrational dynamics is obtained. Systems studied include tungsten hexacarbonyl in the organic glasses 2-methylpentane, 2-methyltetrahydrofuran, and dibutylphthalate, and wild-type and mutant myoglobin-CO in glycerol/water.

INTRODUCTION

To completely understand a vibrational lineshape, a series of experiments is required to characterize the static and dynamic components of the line. These experiments can be performed in the time-domain, where well defined techniques exist for measuring the various quantities. Nonlinear vibrational spectroscopy can be used to eliminate static inhomogeneous broadening from vibrational spectra. Vibrational echo experiments[1-3] can determine the homogeneous vibrational lineshape, which contains the important microscopic dynamics, even when this lineshape is masked by inhomogeneous broadening.

Below, we present the temperature-dependent vibrational dynamics of the T_{1u} CO stretching mode (~1980 cm^{-1}) of tungsten hexacarbonyl ($W(CO)_6$) in the glass-forming liquids 2-methylpentane (2-MP), 2-methyltetrahydrofuran (2-MTHF), and dibutylphthalate (DBP). The temperature dependence of the homogeneous vibrational linewidth in each of the three glassy solvents is T^2, but the behavior is distinct in each of the liquids. The contributions to the vibrational lineshape from different dynamic processes are delineated by combining the results of vibrational echo measurements of the homogeneous lineshape[2] with pump-probe measurements of the lifetime and reorientational dynamics.[3] Further, we present temperature dependent dynamics of the vibrational transition of CO in two proteins, sperm whale myoglobin-CO (MbCO) and a

myoglobin mutant, in which the distal histidine is replaced with a valine (H64V-CO), both in 95%/5% (w:w) glycerol/water. The temperature dependences of the homogeneous vibrational linewidths below the solvent's glass transition show a power law dependence with $T^{1.3}$, but, above the glass transition, the dependence is activated.[4,5]

A measurement of the echo intensity versus time is called an echo decay. The echo decay is related to the fluctuations in the vibrational frequencies, not the inhomogeneous spread in frequencies. The Fourier transform of the echo decay is the homogeneous line shape.[6,7] For example, if the echo decay is an exponential, the lineshape is a Lorentzian with a width, $1/\pi T_2$, where T_2 is obtained from the decay constant.

For a dilute solution of a vibrational chromophore, the homogeneous vibrational linewidth, Γ, has contributions from the rate of population relaxation (lifetime), $1/T_1$, the rate of pure dephasing, $1/T_2^*$, and from orientational relaxation, Γ_{or}. The contributions to the full linewidth at half maximum (FWHM) of the homogeneous line are additive

$$\Gamma = 1/\pi T_2 = 1/\pi T_2^* + 1/2\pi T_1 + \Gamma_{or}. \quad (1)$$

Equation 1 allows the contribution of pure dephasing to the vibrational lineshape to be determined from a knowledge of the homogeneous linewidth, the vibrational lifetime, and the orientational diffusion constant.

The experiments described below were performed using Stanford free electron laser (FEL) as described previously.[4,5] Vibrational echo and pump-probe data were taken on the CO modes of $W(CO)_6$ and Mb-CO, near 5μm. Samples were prepared as reported previously.[5,8]

VIBRATIONAL ECHOES IN LIQUIDS AND GLASSES

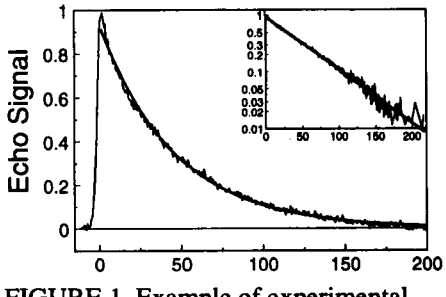

FIGURE 1. Example of experimental data of $W(CO)_6$ in 2MP at 10K.

Figure 1 displays photon echo data for $W(CO)_6$ in 2-MP taken in the low temperature glass at 10 K.[2,8] The inset shows a log plot of the data. The decay is exponential, indicating that the homogeneous line is a Lorentzian. At this temperature, the absorption linewidth is 10.5 cm^{-1} (310 GHz). In contrast, T_2 = 240 ps, yielding a homogenous linewidth of 1.3 GHz. Thus, the absorption line is massively inhomogeneously broadened.

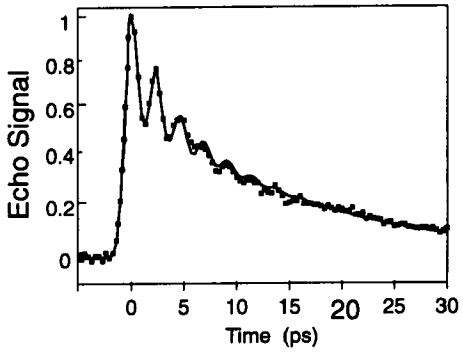

FIGURE 2. Example of beats in the echo signal for $W(CO)_6$ in DBP.

Figure 2 displays data taken using 0.7 ps pulses in the solvent DBP.[3] When the pulse duration is made shorter, the associated bandwidth, Ω, of the transform limited pulse is larger. If the bandwidth of the excitation pulses is comparable to the vibrational anharmonicity, Δ, then population can be excited to higher vibrational levels. For the case where $\Delta \approx \Omega$, short pulse excitation will create a three level coherence involving the v = 0, 1 and 2 vibrational levels. The expected photon echo signal can be described for an unequally spaced three-level system using a semiclassical perturbative treatment of the third-order nonlinear polarizability.[9,10] The three-level system is spaced by the frequencies ω_{10} and ω_{21}, where $\omega_{10} = \omega_{21} + \Delta$, and $\Delta << \omega_{10}$ and ω_{21}. The transition frequencies ω_{10} and ω_{21} lie within the bandwidth of the pulses. For a finite pulse bandwidth, where the E-field amplitude differs at ω_{10} and ω_{21}, the decay is given by[2]

$$I(\tau) = \exp(-2\gamma_{10}\tau)\left[E_{10}^2 \exp(-2\gamma_{10}\tau) + E_{21}^2 \exp(-2\gamma_{21}\tau) - 2\,E_{10}E_{21}\exp(-(\gamma_{10}+\gamma_{21})\tau)\cos(\Delta\tau+\phi)\right]. \quad (2)$$

Here, E_{10} and E_{21} are excitation E-field amplitudes for the v = 0→1 and v = 1→2 transitions, respectively. Equation 2 shows that the echo signal envelope decays in proportion to the dephasing rates of the v = 0→1 and v = 1→2 transitions, with exponentially damped beats observed at the frequency splitting, Δ. The dephasing rates, $1/T_2$, for the two transitions are γ_{10} and γ_{21}.

As can be seen from fig. 2, the decay is consistent with the expected decay of a three level vibrational coherence. The decay is modulated at a 2.3 ps frequency, which is constant within error over all temperatures. Based on the average of several data sets, the vibrational anharmonic splitting is $\Delta = 14.7\ cm^{-1} \pm 0.3\ cm^{-1}$[3]. This splitting is in accord with the value of $15\ cm^{-1} \pm 1\ cm^{-1}$ subsequently obtained by Heilweil and co-workers from observation of the v = 1→2 and v = 2→3 transitions of the asymmetric CO stretching mode of $W(CO)_6$ in hexane using transient infrared absorption.[11] The agreement between the anharmonicity obtained from the beat frequency and that obtained by transient absorption confirms the interpretation of the beats as arising from the multilevel coherence of the anharmonic oscillator. The echo decay data also provide the homogeneous dephasing times for the two transitions involved in the multilevel coherence.[3]

Vibrational echo beat measurements are applicable to many systems.[12] For example, in H64V-CO, a mutant of sperm whale myoglobin, in glycerol/water, beats were measured which showed the dephasing rates of the lower and upper pairs of levels are nearly identical at 10 ps, see fig. 3. The inset is the residual of the data when fit to an exponential. The measured anharmonicity of this transition is at 25.4cm^{-1}. Thus, observations can be made on transitions with significant anharmonicities. Using fs IR pulses, anharmonicities larger than 100 cm^{-1} can be measured.

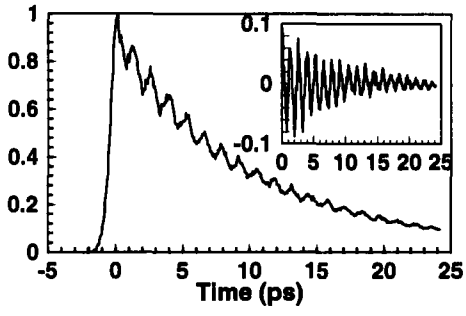

FIGURE 3. Beat decay of H64V-CO in glycerol/water. Inset is the residual to of the data fit to a exponential.

As shown in figure 4a, the temperature dependence of the homogeneous linewidth increases monotonically in the glass. Data is shown in three glassy solvents, 2-MTHF (T_g = 86 K), 2-MP (T_g = 80 K), DBP (T_g = 169 K). The temperature dependences of the homogeneous vibrational linewidths in the three glasses are compared using a reduced variable plot[8] in fig. 4a. Although the absolute linewidths for each system are different, this is a reflection of the strength of coupling of the transition dipole to the bath and can be removed by normalization to the linewidth at the glass transition temperature. Likewise, using a reduced temperature, T/T_g, allows thermodynamic variables that contribute to determining the glass transition to be normalized. Such normalization allows comparison of the functional form of the temperature dependences, independent of differences in T_g and coupling strengths. Figure 4a shows that the temperature dependences of the homogeneous linewidths are identical in the three glasses and are well described by a power law of the form

$$\Gamma(T) = \Gamma_0 + A\,T^{\alpha} \qquad (3)$$

The offset at 0 K, Γ_0, represents the linewidth due to the low temperature vibrational lifetime. A fit to eq. 3 for all temperatures below the glass transition is shown in fig. 4a, and yields an exponent of $\alpha = 2.1 \pm 0.2$. At temperatures

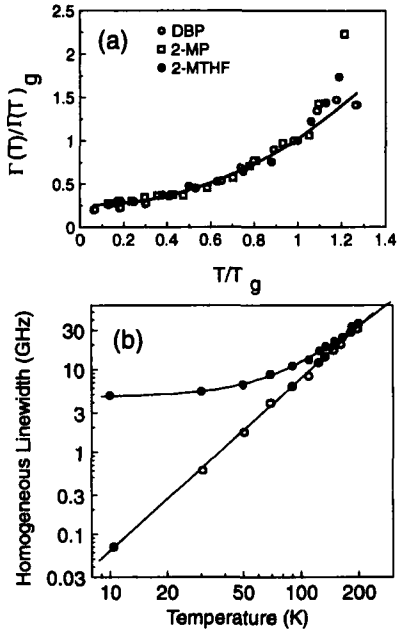

FIGURE 4a. Reduced plot of $W(CO)_6$ in DBP, 2MP and 2MTHF.

FIGURE 4b. Homogeneous Linewidth of $W(CO)_6$ in DBP with and without lifetime contributions.

above ~1.2 T_g, the linewidths of the three liquids diverge from one another. The data from each sample were individually fit to eq. 3. The results demonstrate that the temperature dependence is well described by a power law of the form T^2.

Because of its high glass transition temperature, DBP allows the largest temperature range over which to observe the power law. The data are presented in two ways in fig. 4b. The solid circles are the data and the line through them is a fit to eq. 3. To show more clearly the power law temperature dependence, the open circles are the data with the low temperature linewidth, Γ_0 (corresponding to a vibrational lifetime, $T_1(0\ K) = 33$ ps) subtracted out. The line through the data is T^2. It can be seen that the power law describes the data essentially perfectly over a change of linewidth of ~500 from 10 K to 200 K.

At temperatures above ~1.2T_g, the linewidths of the three liquids diverge from one another. In 2-MP, the vibrational line is homogeneously broadened at room temperature while in DBP it is still massively inhomogeneously broadened, i. e., the homogeneously linewidth is 1 cm^{-1} while the inhomogeneous width is 26 cm^{-1}.

Using the pump-probe measurements of the orientational diffusion, Γ_{or} and the population relaxation time T_1[8,13] the contribution due to pure dephasing can be determined from the homogeneous linewidth.

Figure 5 displays the decomposition of the temperature dependence of the $W(CO)_6$ in 2-MP homogeneous vibrational linewidth into its three dynamic components.[8] At low temperature, where the contributions from pure dephasing and orientational relaxation are negligible, the contribution to the linewidth from the lifetime and the linewidth are equal within error. This is the expected low temperature limit for the homogeneous vibrational linewidth where processes caused by thermal fluctuations disappear, and only lifetime broadening is possible. At high temperatures, the pure dephasing is the dominant contribution. Only between these extremes does orientational relaxation make a contribution to the linewidth, and even then the magnitude of the contribution is relatively small.

The line through the pure dephasing is a power law at low temperature and a Vogel-Tammann-Fulcher form above T_g.

$$\tau = \tau_0 \exp\left(B/(T - T_0)\right) \tag{4}$$

This equation describes a process characterized by a time, τ, with a temperature-dependent activation energy that diverges at a temperature, T_0, below the nominal glass transition temperature. T_0 can be linked thermodynamically to an "ideal" glass transition temperature that would be measured with an ergodic observable.[14] This equation describes the temperature dependence of the viscosity of 2-MP well, and gives $T_0 = 59$ K.[8]

If the VTF equation applies to pure dephasing above the glass transition, then the full temperature dependence would be the sum of the low temperature power law plus a VTF term. To test this idea, the temperature-dependence of pure dephasing was fit to

$$\Gamma^*(T) = A_1 T^{\alpha} + A_2 \exp\left(-B/\left(T - T_0^*\right)\right) \tag{5}$$

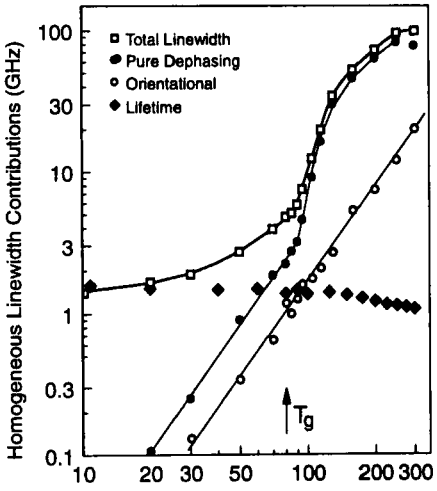

FIGURE 5. Temperature dependent contribution to homogeneous linewidth of $W(CO)_6$ in 2-MP.

for all temperatures below 300 K, and is shown as the line through the pure dephasing data in fig. 5. The fit describes the entire temperature dependence exceedingly well, and yields a reference temperature of $T_0^* = 80$ K. This reference temperature matches the laboratory glass transition temperature T_g exactly, not the ideal glass transition temperature T_0. We can thus infer that the onset of the dynamics that cause the rapid increase in homogeneous dephasing in 2-MP is closely linked with the onset of structural processes near the laboratory glass transition temperature. This may be a manifestation of the short time scale of the measurement and a reflection of the non-ergodicity of the system.

These data represent the first time that each contribution to a vibrational homogeneous line has been independently determined, and the determination is over a broad temperature range.

VIBRATIONAL ECHOES IN PROTEINS

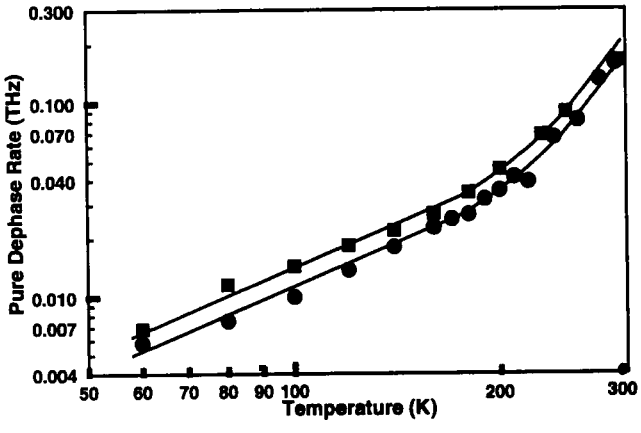

FIGURE 6. Pure dephasing rates of Mb-CO and H64V versus temperature

Figure 5 displays the CO vibrational pure dephasing, T_2^*, of MbCO (squares) and H64V-CO (circles) on a log plot. The temperature dependence of the pure dephasing rates are less steep at low temperatures. There are breaks in the temperature dependences at ~185 K, which is within the range of temperatures associated with the T_g of the glycerol/water solvent. Below this transition, the data fall on a straight line, indicating power law behavior of the form aT^{α}, where $\alpha = 1.3 \pm 0.01$. The dephasing rate for H64V-CO is slower than for the wild type over the entire temperature range.[5]

Above the solvent glass transition, the Mb-CO dephasing dynamics exhibit a clear deviation from the low temperature power law behavior. This change can likely be attributed to the softening of the boundary condition placed on protein motions by the solvent. Above T_g, the temperature dependence fits an activated process. The activation energy is ~1000 cm^{-1}. The $T^{1.3}$ dependence is reminiscent of the temperature dependence that has been observed for the pure dephasing rate of electronic transitions of molecules in low temperature glasses.[15,16] Several experiments suggest a relationship between proteins and glasses.[17-19]

The $T^{1.3}$ temperature dependence observed in Mb-CO can be understood in terms of a tunneling Protein Two Level System (PTLS) model.[4] A protein is a non-equilibrium system with many possible conformations. Conformational changes can be viewed as occurring via motion on a multidimensional potential surface. The PTLS model represents this complex potential surface as a collection of double well potentials, each side representing a different protein conformation. Each protein molecule contains many PTLS, which are associated with the possible conformational changes that can occur. The wells have a variety of energy differences, barrier heights, and tunneling parameters.

Comparing the data points at each temperature reveals that the H64V-CO data is 21% ±3% slower than the wild type data with no systematic variation. It can be seen that within experimental error, the functional form of the two data sets is identical. (The wild type point at room temperature has a large error bar.) These results confirm that CO pure dephasing is caused by coupling to the protein fluctuations since a change in the protein with no change in the solvent produces a substantial change in the rate of pure dephasing.

It was proposed that fluctuating electric fields produced by time dependent protein structural fluctuations are responsible for CO vibrational dephasing in Mb.[4] We have observed that replacing the polar distal histidine with the non-polar valine residue reduces the rate of pure dephasing by ~21% but does not change the temperature dependence. The proteins differ only in a single residue, which replaces the interaction between CO and the polar distal histidine by a weaker interaction between CO and nonpolar valine. Other less significant structural differences, and differences in Mb affinity for CO which arise as a result of this substitution have been discussed in detail in the literature.[20-22] The global dynamics of the protein will not be changed by the substitution of the valine for the distal histidine. Thus, the temperature dependence is unchanged. However, the coupling of the protein fluctuations to the CO vibrational frequency will be reduced because one of the closest sources of the fluctuating electric field has been removed.

CONCLUSION

Analysis of a vibrational lineshape can provide detailed information on dynamics and intermolecular interactions in condensed matter systems. However, to completely characterize an infrared lineshape, a combination of experimental methods is necessary to elucidate each of the dynamic and static contributions to the line. Picosecond

infrared vibrational echo experiments were used to measure the homogeneous lineshape and remove inhomogeneity. Infrared pump-probe experiments were used to measure the vibrational lifetime and orientational relaxation. The total vibrational lineshape was determined by absorption spectroscopy. Together, these experiments yield a complete characterization of the dynamics that make up the homogeneous line, and the extent of inhomogeneity of the infrared absorption spectrum.

Acknowledgments

This body of work could not have been accomplished without a large number of people. Dr. A. Tokmakoff was primarily responsible for all the $W(CO)_6$ measurements. Dr. R. S. Urdahl, Dr. D. A. Zimdars, R. S. Francis, Dr. A.S. Kwok also made significant contributions to the $W(CO)_6$ experiments. Prof. Dana Dlott, Dr. Chris Rella, Dr. Jeffrey Hill contributed significantly to the protein experiments.

REFERENCES

(1) D. Zimdars; A. Tokmakoff; S. Chen; S. R. Greenfield; T.I. Smith, H. A. Schwettman, M. D. Fayer, Phys. Rev. Lett., 70, 2718, (1993)

(2) A. Tokmakoff; D. Zimdars; B. Sauter; R. S. Francis; A. S. Kwok; M. D. Fayer, J. Chem. Phys., 101, 1741, (1994)

(3) A. Tokmakoff; A. S. Kwok; R. S. Urdahl; R. S. Francis; M. D. Fayer, Chem. Phys. Lett., 234, 289, (1995)

(4) C. W. Rella; A. Kwok; K. D. Rector; J. R. Hill; H. A. Schwettman; D. D. Dlott; M. D. Fayer, Phys. Rev. Lett.,77, 1648, (1996)

(5) C. W. Rella; K. D. Rector, A. S. Kwok; J. R. Hill; H. A. Schwettman; D. D. Dlott; M. D. Fayer, J. Phys. Chem., **100,** 38, 15620 (1996)

(6) T. C. Farrar; D. E. Becker *Pulse and Fourier Transform NMR*; Academic Press: New York, 1971.

(7) J. L. Skinner; H. C. Anderson; M. D. Fayer, J. Chem. Phys., 75, 3195, (1981)

(8) A. Tokmakoff; M. D. Fayer, J. Chem. Phys., 102, 2810, (1995)

(9) S. Mukamel; R. F. Loring, J. Opt. Soc. B., 3, 595, (1986)

(10) R. F. Loring; S. Mukamel, J. Chem. Phys., 83, 2116, (1985)

(11) S. M. Arrivo; T. P. Dougherty; W. T. Grubbs; E. J. Heiweil, Chem. Phys. Lett., 235, 247, (1995)

(12) K. D. Rector; C. W. Rella; A. S. Kwok; A. Tokmakoff; M. D. Fayer, in preparation, (1996)

(13) A. Tokmakoff; R. S. Urdahl; D. Zimdars; A. S. Kwok; R. S. Francis; M. D. Fayer, J. Chem. Phys., 102, 3919, (1994)

(14) C. A. Angell, J. Phys. Chem. Solids, 49, 863, (1988)

(15) M. Berg; C. A. Walsh; L. R. Narasimhan; K. A. Littau; M. D. Fayer, J. Chem. Phys., 88, 1564, (1988)

(16) L. R. Narasimhan; K. A. Littau; D. W. Pack; Y. S. Bai; A. Elschner; M. D. Fayer, Chemical Rev., 90, 439, (1990)

(17) R. H. Austin; K. Beeson; L. Eisenstein; H. Frauenfelder; I. C. Gunsalus; V. P. Marshal, Phys. Rev. Lett., 32, 403, (1974)

(18) I. E. T. Iben; D. Basunstein; W. Doster; H. Frauenfelder; M. K. Hong; J. B. Johnson; S. Luck; P. Ormos; A. Schulte; P. J. Steinback; A. Xie; R. D. Young, Phys. Rev. Lett., 62, 1916, (1989)

(19) R. Elber; M. Karplus, Science, 235, 318, (1987)

(20) J. R. Hill; D. D. Dlott; C. W. Rella; K. A. Peterson; S. M. Decatur; S. G. Boxer; M. D. Fayer, J . Phys. Chem., accepted, (1996)

(21) J. R. Hill; D. D. D.; C. W. Rella; T. I. Smith; H. A. Schwettman; K. A. Peterson; A. S. Kwok; K. D. Rector; M. D. Fayer, Biospec., accepted, (1996)

(22) J. R. Hill; D. D. Dlott; M. D. Fayer; C. W. Rella; M. M. Rosenblatt; K. S. Suslick; C. J. Ziegler, J. Phys. Chem., accepted., (1996)